Published in final edited form as:
Dev Dyn. 2011 March ; 240(3): 682–694. doi:10.1002/dvdy.22558.

Dynamic Analysis of BMP-Responsive Smad Activity in Live Zebrafish Embryos

Derek W. Laux, **Jennifer A. Febbo**, and **Beth L. Roman***
Department of Biological Sciences, University of Pittsburgh, Pittsburgh, PA 15260

Abstract

Bone morphogenetic proteins (BMPs) are critical players in development and disease, regulating such diverse processes as dorsoventral patterning, palate formation, and ossification. These ligands are classically considered to signal via BMP receptor-specific Smad proteins 1, 5, and 8. To determine the spatiotemporal pattern of Smad1/5/8 activity and thus canonical BMP signaling in the developing zebrafish embryo, we generated a transgenic line expressing EGFP under the control of a BMP responsive element. EGFP is expressed in many established BMP signaling domains and is responsive to alterations in BMP type I receptor activity and *smad1* and *smad5* expression. This transgenic Smad1/5/8 reporter line will be useful for determining ligand and receptor requirements for specific domains of BMP activity, as well as for genetic and pharmacological screens aimed at identifying enhancers or suppressors of canonical BMP signaling.

Keywords

Zebrafish; Bone Morphogenetic Proteins; Smads; Transgenic Reporter

Introduction

Bone morphogenetic proteins (BMPs), which are members of the transforming growth factor-β (TGF-β) ligand superfamily, play numerous roles in development and disease. For example, in vertebrate development, BMP signaling is required for dorsoventral axis formation and ventral cell fate specification during gastrulation, tailbud and somite formation, cardiomyocyte differentiation, pharyngeal arch development, dorsal retina specification, and upper lip and palate fusion, among other processes (Dosch et al., 1997; Nguyen et al., 1998; Hild et al., 1999; Dick et al., 2000; Bauer et al., 2001; Beck et al., 2001; Mintzer et al., 2001; Payne-Ferreira and Yelick, 2003; Liu et al., 2005; Klaus et al., 2007; French et al., 2009; Marques and Yelon, 2009). Furthermore, disruption of BMP signaling is associated with several human diseases, including pulmonary arterial hypertension, hereditary hemorrhagic telangiectasia, and fibrodysplasia ossificans progressiva (Berg et al., 1997; Deng et al., 2000; Lane et al., 2000; Shore et al., 2006). While this diverse family of more than 20 ligands has been studied in many different contexts, discoveries of functional

*To whom correspondence should be addressed: Beth L. Roman, University of Pittsburgh, Department of Biological Sciences, 4249 Fifth Avenue, Pittsburgh, PA 15260, Phone: 412 383 5297, Fax: 412 624 4759, romanb@pitt.edu.

redundancies, promiscuous receptor binding, and non-canonical downstream effector activation have complicated elucidation of the molecular nature of BMP signaling pathways in specific developmental processes and disease states.

BMPs and other members of the TGF-β superfamily bind as homo- or heterodimers to a heterotetrameric complex consisting of two type II receptors and two type I receptors, both of which are serine/threonine kinases (Feng and Derynck, 2005). Ligand binding facilitates receptor complex formation, allowing the constitutively active type II receptor to phosphorylate the type I receptor within a glycine- and serine-rich (GS) motif. The now-active type I receptor then phosphorylates Smad proteins at a C-terminal SSXS motif (Kretzschmar et al., 1997). Phosphorylation releases these receptor-specific Smads (R-Smads) from an autoinhibitory fold (Hata et al., 1997), allowing them to heterodimerize with the common partner Smad, Smad4, translocate to the nucleus, and, in concert with coactivators and corepressors, regulate transcription of target genes (Ross and Hill, 2008).

Typically, TGF-β, nodal, and activin ligands complex with type I receptors (Alk4, Alk5, or Alk7) that phosphorylate Smads 2 and 3. In contrast, BMPs complex with type I receptors (Alk1, Alk2, Alk3, or Alk6) that phosphorylate Smads1, 5, and 8. The specificity of type I receptor/Smad interaction is governed by the type I receptor L45 loop, and the L3 loop and α-helix1 within the Smad C-terminal MH2 domain (Feng and Derynck, 1997; Chen et al., 1998; Lo et al., 1998; Persson et al., 1998; Chen and Massague, 1999). More recently, TGF-β has been shown to induce Smad1/5 phosphorylation in many different cell types (Liu et al., 1997; Goumans et al., 2002; Pannu et al., 2007; Bharathy et al., 2008; Daly et al., 2008; Liu et al., 2009; Wrighton et al., 2009), whereas BMP9 has been shown to induce Smad2 phosphorylation in endothelial cells (Upton et al., 2009). In some cases, these seemingly non-canonical responses are actually dependent on canonical type I receptor/Smad interactions, with TGF-β inducing the formation of mixed complexes containing both Smad2/3- and Smad1/5-specific type I receptors (Goumans et al., 2003; Daly et al., 2008). However, in other cases, these responses seem to rely instead on novel activities of type I receptors, with Smad1/5-specific receptors phosphorylating Smad2, and Smad2/3-specific receptors phosphorylating Smad1/5 (Liu et al., 2009; Upton et al., 2009; Wrighton et al., 2009). These findings challenge the notion of type I receptor Smad specificity and introduce further complexity into TGF-β family signaling pathways.

Phosphorylated R-Smad/Smad4 complexes regulate gene expression by binding to specific sequences within DNA and recruiting co-activators or co-repressors. While the specificity of DNA binding is not fully understood, it is clear that TGF-β-responsive Smads and BMP-responsive Smads activate different sets of genes. For example, phosphorylated Smad3 (pSmad3)/Smad4 binding to Smad Binding Elements (SBEs; GTCT) in the *plasminogen activator inhibitor-1* (*PAI-1)* promoter is required for TGF-β-induced gene expression, and SBE multimers, in concert with a minimal promoter, confer responsiveness to TGF-β (Dennler et al., 1998). In contrast, pSmads1, 5, and 8 can, in concert with Smad4, induce expression of *inhibitor of differentiation-1* (*Id1*) via binding to specific sites in its promoter (Korchynskyi and ten Dijke, 2002; Monteiro et al., 2004). A so-called BMP responsive element (BRE) containing two regions of the mouse *Id1* promoter (−1052 to −1032; −1105 to −1080), ligated together and arranged as an inverted repeat, confers BMP responsiveness

to a minimal promoter (Korchynskyi and ten Dijke, 2002). However, pSmad1/Smad4 can also regulate gene expression independently of canonical BMP responsive elements, either by binding directly to noncanonical *cis* elements (Mandel et al., 2010) or by interacting with non-Smad transcription factors to mediate gene expression through their cognate *cis* elements (Zhao et al., 2003; Wang et al., 2007).

BMP signaling is negatively regulated at multiple levels, including ligand sequestration by soluble antagonists such as chordin and noggin; competition between R-Smads and inhibitory Smads (Smads 6 and 7) for binding to type I receptors or to Smad4; phosphatase-mediated dephosphorylation of type I receptors and R-Smads; ubiquitination and degradation of type I receptors, R-Smads, and Smad4; phosphorylation of Smads at sites other than the SSXS motif; and availability of nuclear co-activators and co-repressors (Itoh and ten Dijke, 2007). Therefore, while BMP ligand, BMP receptor, and Smad expression patterns are informative, expression of pathway components cannot be equated with BMP activity. To better localize canonical BMP activity during development, BMP reporter mice have been generated that express β-galactosidase or GFP under the control of a BRE (Monteiro et al., 2004; Blank et al., 2008; Monteiro et al., 2008). These models define sites of Smad1/5/8-mediated transcription in developing mice, including the dorsal optic vesicle, midbrain and hindbrain, anterior branchial arches, forelimb bud, heart, and tail mesenchyme at E9.5; and forebrain, snout, trigeminal ganglia, dorsal root ganglia, gut, kidney, liver, lung, heart, vasculature, skin, and limb at later stages. Generally, these domains correspond to the presence of pSmad1/5. To our knowledge, these models have not been exploited to determine ligand or receptor dependence of these activity domains, nor have they been used to identify novel genes or small molecules that impinge upon BMP signaling.

To expand the repertoire of models available for studying BMP signaling in vivo, we generated a transgenic zebrafish Smad1/5/8 reporter line using the BRE, in concert with a minimal promoter, to drive expression of EGFP. *Tg(bre:egfp)* embryos express EGFP in multiple domains known to require BMP activity, and EGFP expression is responsive to both activation and inhibition of Smad1/5 phosphorylation, suggesting that EGFP expression faithfully reports BMP activity. Because zebrafish embryos are externally fertilized, transparent, and undergo rapid embryogenesis, this zebrafish BMP reporter line will allow mapping of endogenous BMP signaling over the course of development in live animals. Furthermore, because they are amenable to embryonic manipulations such as overexpression and knockdown, they can be used to define ligand-, receptor-, and Smad-dependence of different activity domains. Finally, *Tg(bre:egfp)* embryos can be used in genetic and chemical screens to identify novel players that either enhance or inhibit BMP signaling, either globally or in specific domains. These attributes may allow discovery of small molecules with specificity for particular ligands, receptors, or Smads involved in BMP signaling, providing finely-tuned tools for probing specific developmental processes and targeting specific BMP-related diseases.

RESULTS

Generation of transgenic zebrafish lines expressing EGFP under the control of a BRE

We assembled a DNA construct containing a BRE upstream of an adenovirus minimal *e1b* promoter and carp *β-actin* transcriptional start site (Scheer and Campos-Ortega, 1999), followed by EGFP coding sequence and a polyA signal. This construct, flanked by *Tol2* transposon arms (Kawakami et al., 2004; Urasaki et al., 2006), was injected along with transposase mRNA into one-cell stage zebrafish embryos. Transient expression was observed in many structures that proved positive in stable transgenics (detailed below), whereas injection of a similar construct lacking the BRE was silent (data not shown). We identified 13 P0 founders, which ranged in germline transmission rates from 3–92%. Careful examination of two independent F1 lines, *Tg(bre:egfp)*^{pt509} (Fig. S1) and *Tg(bre:egfp)*^{pt510} (Fig. 1), revealed identical patterns of EGFP expression, suggesting that expression domains are not reflective of the genomic context of the insertion.

bre:egfp expression correlates with many established domains of BMP activity

EGFP expression is first faintly detectable in the tailbud of developing *Tg(bre:egfp)* embryos at the 6 somite (6s) stage (12 hours post-fertilization or hpf; Fig. 1a). While expression in this domain is weak at 6 somites, it is quite strong in the tailbud and has extended into the developing tail somites by the 12 somite stage (15 hpf; Fig. 1b). The presence of BMP activity in the tailbud and somites correlates with expression of *smad1* and *smad8* and presence of pSmad1/5/8 in zebrafish, and corroborates the established role for BMP signaling in zebrafish tailbud and somite development (Muller et al., 1999; Thisse and Thisse, 2004; Row and Kimelman, 2009). A second early expression domain in 12s *Tg(bre:egfp)* embryos resides in the presumptive myeloid progenitor domain, just caudal to the eye (Fig. 1b). By the 18s stage (18 hpf; Fig. 1c), EGFP-positive myeloid cells can be seen migrating bilaterally away from their origin. Expression in this domain corroborates the established requirement for *smad1* in zebrafish macrophage and granulocyte development (McReynolds et al., 2007).

By 1 day post-fertilization (dpf), BRE activity has expanded to many new domains (Fig. 1d), including the heart (Fig. 1g–i). At this time, the entire endocardium is strongly EGFP-positive, colocalizing with *fli1a*-driven dsRed expression in both the atrium and ventricle (Fig. 1g–g″). Sparse expression is also evident in the myocardium, which surrounds the endocardium (Fig. 1g, g′). By 2 dpf, this expression pattern has inverted, with EGFP expressed most strongly in myocardial cells, as evidenced by colocalization with *myosin light chain 7* (*myl7)*-driven nuclear-dsRed, and more weakly in endocardial cells, as evidenced by minimal colocalization with *fli1a*-driven dsRed (1e, h–h″). Between 2 and 3 dpf (data not shown), expression wanes in the endocardium to nearly undetectable levels and coalesces within the myocardium to the level of the atrioventricular canal, persisting in this pattern until at least 4 dpf (Fig. 1f, i–i″). *BRE*-driven transgene expression in mice (Blank et al., 2008) and pSmad1 expression in chick (Faure et al., 2002) have been reported in both endocardium and myocardium, and expression in these domains corroborates known roles of BMP signaling in endocardial cushion formation (Wang et al., 2005; Choi et al., 2007),

cardiomyocyte survival (Gaussin et al., 2002), and cardiomyocyte-specific *tbx20* expression (Mandel et al., 2010).

Moving posteriorly from the heart, another strong domain of *bre*-driven EGFP expression is encountered in ventrolateral regions of the pharyngeal arches at 1 dpf (Fig. 1d, j, j′). At this time, no segmentation is evident, whereas by 2 dpf, segmentation delineates ventrolateral regions of each pharyngeal arch (Fig. 1e, k, k′). By 3 dpf (not shown), pharyngeal expression is no longer bilateral but instead has coalesced at the ventral midline, with expression persisting in this midline domain until at least 4 dpf (Fig. 1f, l–l‴). Closer examination reveals two distinct EGFP expression domains within the ventromedial pharyngeal arches. One domain surrounds and is closely apposed to the ventral aorta (Fig. 1l′–l″), and is likely vascular smooth muscle, which first appears in this region around 3–4 dpf (Santoro et al., 2009). The second, segmented domain is more ventral and likely corresponds to the medial basihyal and basibranchial/hypobranchial cartilages (Fig. 1l‴). Pharyngeal arch expression correlates with reported expression of *bre*-driven GFP in mouse pharyngeal arches (Monteiro et al., 2004) and corroborates the established role of BMP signaling in development of zebrafish pharyngeal arches (Payne-Ferreira and Yelick, 2003).

bre-driven EGFP is expressed in the dorsal retina at 1 dpf (Fig. 1d, m, m′), but is no longer detectable by 2 dpf (Fig. 1e) This expression domain corroborates the established requirement for GDF6a (BMP-13)-mediated signaling in zebrafish dorsal retina specification (French et al., 2009). Just caudal to the eyes, the trigeminal ganglia also express EGFP at 1 dpf (Fig. 1m, m″), with expression intensifying over the course of the day and persisting until at least 4 dpf. In mice, dorsal trigeminal neuron identity requires cell-autonomous BMP activity (Hodge et al., 2007), supporting our observation that only dorsal axonal projections emanating from this ganglion report pSmad1/5-mediated EGFP expression in zebrafish. Additional anterior domains of BRE-mediated EGFP expression at 1 dpf include the pineal gland/epiphysis (Fig. 1d, n), which lies at the midline of the dorsal diencephalon and functions as a circadian pacemaker; and the ventral diencephalon, or hypothalamic rudiment (Fig. 1d, o). Expression in these domains is also transient, waning during day 2. While we could find no published role for BMP signaling in the pineal gland, this structure is known to express *id1*, the gene from which the BRE was derived, in rat and zebrafish (Kofler et al., 2002; Toyama et al., 2009). Furthermore, BMP signaling is known to be required for hypothalamic patterning in chick embryos (Manning et al., 2006). Thus, these two domains would be expected to report pSmad1/5 activity.

In the trunk and tail of 1 dpf *Tg(bre:egfp)* embryos, EGFP is expressed in the most ventral aspect of the embryos, including the mesenchyme underlying the yolk extension and the forming common kidney/gastrointestinal opening, the cloaca (Fig. 1d, p, p′). Cloacal expression wanes over the course of the day, decreasing from a peak around the 26–28 somite stage (22–23 hpf). Interestingly, cloacal expression re-appears at 3–4 dpf (Fig. 1f, q, q′). Expression timing correlates with connection of the kidney tubules (28 somites) and gut tube (4 dpf) to this common opening, and supports the established role of BMP signaling in cloacal development (Pyati et al., 2006). Also in the trunk, EGFP continues to be expressed in the somites through 4 dpf (Fig. 1d–f, r, r′). While the intensity of EGFP expression in this domain decreases between 1 and 2 dpf, expression increases between 2 and 3 dpf and

remains strong in most embryos at 4 dpf. The somitic expression domain is the most variable domain in *Tg(bre:egfp)*^{pt510}, with approximately 90 and 70% showing intermediate to strong somite expression at 1 and 4 dpf, respectively.

bre-driven EGFP expression continues at 2 dpf in the heart, pharyngeal arches, trigeminal ganglia, pineal gland, hypothalamus, and somites, as described above. In addition, clear expression is now evident in the developing mouth opening, or stomodeum, within the first pharyngeal arch (Fig. 1s). The dorsoanterior expression domain of the stomodeum represents the maxillary process, whereas the ventroposterior expression domain of the stomodeum represents the mandibular process, which together delineate the forming mouth opening. Weaker expression is also seen in an adjacent horseshoe-shaped, slightly more dorsal-anterior domain that follows the contours of the ventral diencephalon (Fig. 1s). The maxillary and mandibular processes thin along the dorsoventral axis and elongate along the left/right axis by 4 dpf to form the mouth opening (Fig. 1t). Interference with BMP signaling results in cleft lip and cleft palate in mice, suggesting a critical conserved role for BMP-mediated pSmad1/5 activity in oral cavity development (Liu et al., 2005).

At 2 dpf, *bre*-driven EGFP expression is also strong in the pectoral fin bud, at the base of the fin as well as at the apical ectodermal ridge (Fig. 1e, u). This expression domain is substantiated by the requirement for BMP signaling through the type I receptor, Alk8 (homologous to mammalian ALK2), in pectoral fin development (Liu and Stainier, 2010). Additionally, strong EGFP expression is apparent in many cells in the median fin fold, particularly in the ventral region (Fig. 1e, v). These cells have a dendritic appearance similar to that described for neural crest-derived mesenchymal cells that give rise to fin rays, or lepidotrichia (Smith et al., 1994). Finally, several spinal cord neurons are EGFP-positive at 2 dpf (Fig. 1w). Cell bodies are positioned approximately at the midline, midway along the dorsoventral axis of the spinal cord, and axons extend bidirectionally, parallel to the anterior/posterior axis. Pectoral fin, median finfold, and spinal neuron *bre*-driven EGFP expression domains persist until at least 4 dpf.

Temporal correlation between pSmad1/5/8 expression and *bre*-driven EGFP fluorescence

Because EGFP takes time to fold and fluoresce and is a stable protein (Corish and Tyler-Smith, 1999), the temporal pattern of EGFP fluorescence in *Tg(bre:egfp)* embryos would not be expected to precisely reflect the temporal activity of pSmad1/5/8. To gauge the offset between pSmad1/5/8 activity and transgene expression, we assessed pSmad1/5/8 expression, e*gfp* mRNA expression, and EGFP fluorescence in the dorsal retina, a relatively transient EGFP expression domain, between 10 and 38 hpf (Fig. S2). pSmad1/5/8 expression first appears in the dorsal retina at 12 hpf, e*gfp* mRNA at 14 hpf, and EGFP fluorescence at 16 hpf, demonstrating an approximately four hour delay between the appearance of pSmad1/5/8 and EGFP fluorescence. A similar delay was seen in the trigeminal ganglia (Fig. S2) and heart (data not shown) and in other zebrafish transgenic studies (Jusuf and Harris, 2009). By 28–30 hpf, pSmad1/5/8 and *egfp* mRNA are barely detectable in the dorsal retina, while EGFP fluorescence disappears between 36 and 38 hpf (Fig. S2). Thus, EGFP perdures in this domain for approximately eight-to-ten hours after pSmad1/5/8 is lost. While this perdurance is short compared to other published work demonstrating EGFP stability in vivo

on the order of a day or even weeks (Verkhusha et al., 2003), nearly all *bre*-driven EGFP expression domains are either dynamic or transient, suggesting that in these domains, EGFP is either less stable than previously described or that cell turnover is high.

bre:egfp transgene expression is responsive to changes in Smad1/5/8 phosphorylation

While EGFP expression in *Tg(bre:egfp)* embryos correlates well with known domains of BMP activity, we sought to further validate this model by manipulating phosphorylation of BMP-responsive Smads and assaying effects on EGFP expression. In shield stage *Tg(bre:egfp)* embryos, we can only faintly and variably detect EGFP via fluorescence or in situ hybridization, though pSmad1/5/8 is detectable by immunohistochemistry (Fig. 2a–c). However, injection of one- to two-cell embryos with 5 pg mRNA encoding a constitutively active form of the zebrafish BMP type I receptor, Alk1 ($Alk1^{CA}$), induces EGFP expression at shield stage, as visualized by fluorescence and by in situ hybridization, correlating with a marked increase in nuclear-localized pSmad1/5/8 (Fig. 2d–f). In contrast, injection of up to 100 pg mRNA encoding a constitutively active form of the zebrafish TGF-β type I receptor, Alk5 ($Alk5^{CA}$), fails to induce *bre:egfp* transgene expression or phosphorylation of Smad1/5/8 (Fig. 2g–i), consistent with this receptor's established propensity to phosphorylate Smad2/3.

To further confirm that *bre:egfp* transgene expression is dependent upon BMP signaling, we treated embryos at tailbud stage (10 hpf) with 10 μM dorsomorphin, a small molecule that inhibits BMP type I receptor-mediated Smad1/5/8 phosphorylation (Yu et al., 2008). Treatment at this time avoids dorsalization resulting from treatment prior to gastrulation, allowing us to assess transgene expression during organogenesis. Dorsomorphin treatment reduced EGFP expression in all domains at 1 dpf, most notably in the retina, hypothalamus, heart, pharyngeal arches, somites, and cloaca (Fig. 3e, f, i–r and Table 1), without greatly affecting general morphology (Fig. 3a, b). Furthermore, treatment with 10 μM DMH1, a more potent dorsomorphin analog that, unlike dorsomorphin, does not affect vascular endothelial growth factor receptor (VEGFR) activity (Hao et al., 2010), essentially eliminated EGFP expression in all domains (Fig. 3c, g), whereas treatment with 200 μM SB-431542, an Alk4/5/7 inhibitor, had no effect on EGFP expression (Fig. 3d, h). Taken together with $alk1^{CA}$ overexpression studies, these results demonstrate that the *bre:egfp* transgene is indeed specifically responsive to pSmad1/5/8, and not pSmad2/3.

bre:egfp transgene expression is decreased by knockdown of *smad1* or *smad5*

To further analyze the dependence of *bre*-driven EGFP on *smad1* and *smad5* , we knocked down expression of each of these genes in zebrafish embryos using translation blocking morpholino-modified antisense oligonucleotides (morpholinos). Injection of 4 ng *smad5* morpholino severely dorsalized embryos [C4 phenotype (Mullins et al., 1996)], precluding later analysis (Fig. S3). Injection of 2 ng *smad5* morpholino resulted in slight tail truncations but had little effect on EGFP expression in most domains at 1 dpf, with substantial decreases observed only in the somites and moderate to minimal decreases in dorsal retina and cloaca (Fig. S3 and Table 1). These results demonstrate that *bre*-driven EGFP expression in somites, retina, and cloaca is most sensitive to *smad5* levels. However, since knockdown in

these experiments is incomplete, we cannot make strong conclusions regarding the role of *smad5* in other *bre*-driven EGFP expression domains.

In contrast to the limited effect of *smad5* knockdown on organ-specific *bre*-driven EGFP expression, *smad1* knockdown dampened EGFP expression in many domains (Fig. 4, S4, and Table 1). Injection of 2 ng *smad1* morpholino resulted in moderate to substantial decreases in transgene expression in the dorsal retina (Fig. 4e, f) and hypothalamus (Fig. 4h, i) at 1 dpf, and the stomodeum (Fig. 4k, l) and pectoral fin (Fig. 4n, o) at 2 dpf. These affected domains correlated well with the presence of *smad1* transcripts (Fig. 4g, j, m, p). EGFP expression in *smad1* morphants was also substantially decreased in the cloaca at 1 dpf, and somites and median finfold at 2 dpf (Fig. S4 and Table 1). However, these expression domains did not correlate well with *smad1* mRNA expression, likely due at least in part to EGFP perdurance (Fig. S2). Additional domains showing minimal decreases in EGFP fluorescence included the heart, pharyngeal arches, pineal gland, and somites at 1 dpf; and the pharyngeal arches at 2 dpf (Table 1). The inability of *smad1* knockdown to completely abrogate EGFP expression in any domain suggests either incomplete knockdown or a partial redundancy with *smad5*, which is nearly ubiquitously expressed, and/or *smad8*, which is expressed in the majority of EGFP-positive domains (Thisse and Thisse, 2004). While it is possible that combined *smad1*/*5* knockdown might severely decrease *bre*-driven EGFP expression in many domains, we could not test this possibility because severe developmental defects precluded analysis (data not shown).

Discussion

We have generated a stable transgenic zebrafish line, *Tg(bre:egfp)*, which reports pSmad1/5-mediated transcriptional activation in vivo. Support for this assertion includes a correlation between EGFP expression domains and published requirements for BMP signaling in development of these same cells or tissues; demonstrated sensitivity to modulation of BMP type I receptor activity; and demonstrated correlation with *smad1* expression and sensitivity to *smad1* knockdown. Because BMP signaling is negatively regulated at multiple levels – for example, dephosphorylation of receptors and Smads, I-Smad interference with type I receptor/Smad binding or R-Smad/Smad4 binding, and Smad binding to co-repressors – expression patterns of BMP receptors and Smads cannot accurately predict sites of BMP-mediated transcriptional activity (Itoh and ten Dijke, 2007). Our *Tg(bre:egfp)* line overcomes this limitation inherent in the analysis of simple expression patterns by directly reporting pSmad1/5-mediated transcriptional activity, and can therefore be used as a tool to define cells that respond to BMP signals over the course of development. It should be noted that phosphorylated BMP R-Smad/Smad4 complexes can regulate gene expression independently of canonical *Bre* sites, either by binding directly to unrelated *cis* elements (Mandel et al., 2010) or by interacting with non-Smad transcription factors to mediate gene expression through their cognate *cis* elements (Zhao et al., 2003; Wang et al., 2007). However, the mouse *Id1*-derived BRE used to generate our transgenic reporter line is pSmad1/5-responsive in vitro and in vivo in many different cell types (Korchynskyi and ten Dijke, 2002; Monteiro et al., 2004; David et al., 2007a; Blank et al., 2008; Monteiro et al., 2008) and is postulated to require no additional transcription factor binding partners for activity (Blank et al., 2008). Therefore, while EGFP expression in our *Tg(bre:egfp)* line may

not reflect endogenous binding and activation of “canonical” *Bre* sites, it should report the presence of all nuclear phosphorylated BMP R-Smad/Smad4 complexes, regardless of which *cis*-acting element is being activated within each domain in vivo.

Transgene expression in *Tg(bre:egfp)* embryos is observed primarily within domains with reported requirements for BMP signaling. For example, EGFP is expressed in the dorsal retina, the specification of which requires GDF6a (BMP-13)-mediated Smad1/5 phosphorylation within retinal cells (French et al., 2009). And EGFP is expressed in the forming mouth opening or stomodeum, likely reflecting a requirement for BMP signaling in lip development, as has been previously demonstrated in mice (Liu et al., 2005). However, the role of BMP signaling in other EGFP-positive domains is less clear. For example, to our knowledge, a requirement for BMP-induced Smad1/5 activity in pineal gland development or function has not been reported, although this structure is known to express the Smad1/5-responsive gene, *id1* (Toyama et al., 2009), as well as *bmp2a* (Thisse and Thisse, 2004). Similarly, while we observe strong EGFP expression in putative osteogenic mesenchymal cells in the median finfold, we could find no reports of a requirement for BMP signaling specifically within these cells. Thus, we have defined two previously unidentified domains in which BMP signaling is active during zebrafish embryonic development. Given that *Tg(bre:egfp)*^{pt509} and *Tg(bre:egfp)*^{pt510} showed identical EGFP expression patterns, and that EGFP expression in nearly all domains was decreased by dorsomorphin treatment or *smad1* or *smad5* morpholino injection and eliminated (at 1 dpf) by DMH1 treatment, it is highly unlikely that expression domains reflect insertional artifacts or expression via cryptic enhancers within our *bre:egfp* construct. The only domain that we cannot say with certainty is not artifactual is the 2 dpf spinal cord neurons, which was not affected by *smad1* morpholino but not assayed in drug or *smad5* morpholino experiments.

While *bre*-driven EGFP expression was observed in many anticipated domains in our transgenic line, some structures were unexpectedly negative, despite convincing evidence in the literature for a role for BMP signaling in specification and/or function. For example, while *smad5* is clearly required for gastrulation (Hild et al., 1999; Kramer et al., 2002) and pSmad1/5/8 is detectable ventrally in shield stage embryos, *bre*-driven EGFP expression was undetectable in this domain. Also, while the BMP type I receptor, Alk1, is expressed exclusively in particular arteries in zebrafish embryos and loss of function results in enlarged vessels and arteriovenous malformations (Roman et al., 2002), we could not detect EGFP expression in *alk1*-positive vessels (data not shown). Finally, BMP signaling during somitogenesis promotes pronephric cell fates and inhibits blood and vascular differentiation (Gupta et al., 2006), but we could not detect EGFP expression in the posterior lateral or intermediate mesoderm or their derivatives (data not shown). These examples highlight the limitations of this transgenic reporter approach. The lack of detection of EGFP in the ventral region of shield stage embryos is likely due to the fact that temporal transgene expression patterns do not precisely reflect endogenous BMP activity due to delayed EGFP fluorescence (Fig. S2). In domains in which the effectors of BMP signaling are less clear, the reasons for the lack of EGFP expression could be manifold. Because the BRE used to drive transgene expression may not efficiently report pSmad8/Smad4-mediated gene expression (Monteiro et al., 2004), it is possible that Smad8 is the major effector in

unexpectedly negative domains. Alternatively, these cells may engage non-traditional Smad pathways downstream of receptor activation. For example, TGF-β binding to a non-canonical receptor complex containing both Smad1/5-specific and Smad2/3-specific type I receptors can generate mixed pSmad1/pSmad2 complexes (Daly et al., 2008); BMP9, acting through Alk1, can activate Smad2 phosphorylation (Upton et al., 2009); and ligand-induced R-Smad activation can enhance microRNA processing in a Smad4-independent, post-transcriptional manner (Davis et al., 2008). None of these pathways results in BRE activation. Another possible explanation for the lack of EGFP expression in established BMP activity domains is that Smad-independent pathways might relay signals downstream of BMP type I receptors. For example, in endothelial cells, Alk1 may signal at least in part through MAP kinases (Jadrich et al., 2006; David et al., 2007b). Finally, as BMP signaling can both activate and repress transcription, it is possible that co-repressors present within these unexpectedly negative domains prevent pSmad1/5-mediated *bre:egfp* transactivation. For example, a pSmad1/5-responsive element derived from the *Xenopus laevis Vent2* promoter can mediate heterologous gene activation or repression, depending on the presence of trans-acting co-activators or co-repressors (Yao et al., 2006). However, other reports suggest that pSmad-mediated transcriptional repression occurs in a non-BRE-dependent manner (Liu et al., 2001; Kang et al., 2005), which could not account for the lack of *bre*-driven EGFP expression in anticipated domains.

In summary, we have generated and validated a transgenic zebrafish line that reports pSmad1/5-mediated transcriptional activation. Using genetic approaches, this BMP reporter line can be used to define ligand, receptor, and Smad requirements within individual BMP signaling domains, as we demonstrated using *smad1* morpholinos. Furthermore, these fish can be used to screen for small molecule modulators of BMP signaling, as we demonstrated using dorsomorphin and DMH1, or to screen for genetic modulators of BMP signaling. Besides the obvious advantages of screening for BMP inhibitors in an intact animal model, the *Tg(bre:egfp)* line affords the possibility of uncovering novel drugs with particular BMP ligand or BMP receptor specificity – based on effects within select expression domains – in a single, high content assay. These drugs could prove useful in targeting specific disorders of BMP signaling.

Experimental Procedures

Zebrafish maintenance

Adult zebrafish (*Danio rerio*) were maintained according to standard procedures (Westerfield, 1995). Embryos were raised and staged as described (Kimmel et al., 1995; Westerfield, 1995). For imaging beyond 24 hpf, embryo medium was supplemented with 0.003% phenylthiourea (Sigma) at 24 hpf to prevent melanin formation (Westerfield, 1995).

Generation of *Tg(bre:egfp)*

Multisite Gateway cloning (Invitrogen) was used to generate a *bre:egfp* construct. The BRE is a synthetic palindromic sequence derived from fusing distinct regions of the mouse *Id1* promoter (Korchynskyi and ten Dijke, 2002) and is as follows: 5′-CTAGCTCAGACCGTTAGACGCCAGGACGGGCTGTCAGGCTGGCGCCGCGGCGCC

AGCCTGACAGCCCGTCCTGGCGTCTAACGGTCTGAGCTAG-3′. The *Bre* was released from *BRE:luc* (Korchynskyi and ten Dijke, 2002) by NheI digest; ends were filled in using Klenow; and the blunt product was ligated into the SnaBI site in the 5′ entry clone, *p5E-basprom*, just upstream of a minimal adenovirus *e1b* promoter and carp *β-actin* start site (Scheer and Campos-Ortega, 1999; Villefranc et al., 2007). This clone was then recombined with *pME-egfp* , *p3E-pA*, and *pdesttol2pA2* from the Tol2 kit (Kwan et al., 2007) via standard Multisite Gateway procedures (Invitrogen). Twenty-five pg of the resulting clone, *ptol2-bre:egfp*, was injected into one-cell stage embryos along with 25 pg *transposase* mRNA to effect transposon-mediated transgenesis (Kawakami et al., 2004). Embryos were sorted for EGFP expression and raised to adulthood. Founders were identified by incrossing followed by outcrossing to *Tg(fli1ep:dsRedEx)*^{um13}, which expresses dsRed specifically in endothelial cells (Villefranc et al., 2007; Covassin et al., 2009). Thirteen *Tg(bre:egfp)* founders were identified, and two F1 lines (pt509, pt510) were established from two independent founders.

Imaging

For confocal microscopy, embryos were anesthetized using 0.016% Tricaine (Sigma), mounted in 500 μm troughs in a 2% agarose bed, and Z-series of frame-averaged optical sections were generated using a FluoView500 or FluoView1000 laser scanning confocal microscope (Olympus) outfitted with a 40x water immersion objective. Two-dimensional projections were generated using ImageJ version 1.43 (NIH). For imaging of transgene expression in the heart, *Tg(bre:egfp)*^{pt510} fish were crossed to *Tg(-5.1myl7:nDsRed2)*^{f2} fish, which express nuclear-localized DsRed in myocardial cells. Low power brightfield and fluorescent images were captured using an MVX-10 MacroView macro zoom fluorescence microscope equipped with a DP71 camera (Olympus). Images were compiled using Adobe Photoshop CS2 9.0.2.

mRNA synthesis, morpholinos, and drug treatment

pCS2+ constructs containing constitutively active zebrafish *alk1* and *alk5* (Roman et al., 2002; Park et al., 2008) were used to synthesize capped sense mRNA using SP6 polymerase (mMessage mMachine, Ambion). mRNA was injected into one- to two-cell stage zebrafish embryos, and translation was confirmed by detection of C-terminal myc tags via immunohistochemistry (data not shown). Morpholinos targeting the translation start site of *smad1* and *smad5* (GeneTools) were as follows: *smad1*, 5-AGGAAAAGAGTGAGGTGACATTCAT-3′; *smad5*, 5′-ACATGGAGGTCATAGTGCTGGGCTG-3′. Morpholino sequences were identical to those used in published work (McReynolds et al., 2007), and each morpholino produced expected phenotypes of dorsalization (4 ng *smad5* morpholino) and brain necrosis and yolk extension defects (2 ng *smad1* morpholino) (Hild et al., 1999; McReynolds et al., 2007). The standard control morpholino (GeneTools) was: 5′-CCTCTTACCTCAGTTACAATTTATA-3′. To inhibit type I receptor-mediated Smad phosphorylation, embryos were dechorionated and exposed to 0.5% DMSO (vehicle control), 10 μM dorsomorphin (BMP type I receptor inhibitor; Calbiochem), 10 μM DMH1 (BMP type I receptor inhibitor; gift of Dr. Charles Hong, Vanderbilt University), or 200 μM SB-431542 (TGF-β type I receptor inhibitor; Tocris) beginning at 10 hpf. Exposure to 10 μM dorsomorphin or 5 μM DMH1 beginning at

the one-cell stage resulted in severe dorsalization (Yu et al., 2008), whereas 100 μM SB-431542 resulted in cyclopia (Park et al., 2008), demonstrating that these drugs work as expected in our hands.

In situ hybridization and immunohistochemistry

PCR-amplified fragments of *smad1* and *egfp* were inserted into pCRII-TOPO (Invitrogen) and plasmids used to generate digoxigenin-labeled antisense riboprobes (DIG RNA Labeling Kit, Roche). In situ hybridization was performed as previously described (Hauptmann and Gerster, 1994). Whole mount immunohistochemistry was performed as previously described (Anderson et al., 2008) except blocking solution was 10% fetal bovine serum/1% DMSO/0.1% tween in PBS. Rabbit anti-phospho-Smad1/5/8 (Cell Signaling Technology, #9511) was used at 1:100, and goat-anti-rabbit Alexa Fluor 488 (Invitrogen) at 1:500.

Supplementary Material

Refer to Web version on PubMed Central for supplementary material.

Acknowledgments

We thank Ashley Miller for technical assistance; Zachary Kupchinsky for excellent fish care; Simon Watkins, Greg Gibson, and Jason Devlin (University of Pittsburgh, USA) for access to the Center for Biologic Imaging; Richard Pestell (Thomas Jefferson University, USA) for the *pBRE-luc* construct; Nathan Lawson (University of Massachusetts Medical School, USA) for the *p5Ebasprom* clone and *Tg(fli1ep:dsRedEx)*^{um13} fish; Geoffrey Burns (Massachusetts General Hospital, USA) for *Tg(-5.1myl7:nDsRed2)*^{f2} fish; Koichi Kawakami (National Institute of Genetics, Japan) for permission to use Tol2-mediated transgenesis in zebrafish; Chi-Bin Chen (University of Utah, USA) for the Tol2 kit, and Charles Hong (Vanderbilt University) for DMH1.

Grant information: National Institutes of Health 5R01HL79108; HHMI Undergraduate Science Education Program Grant 52005906.

References

Anderson MJ, Pham VN, Vogel AM, Weinstein BM, Roman BL. Loss of unc45a precipitates arteriovenous shunting in the aortic arches. Dev Biol. 2008; 318:258–267. [PubMed: 18462713]

Bauer H, Lele Z, Rauch GJ, Geisler R, Hammerschmidt M. The type I serine/threonine kinase receptor Alk8/Lost-a-fin is required for Bmp2b/7 signal transduction during dorsoventral patterning of the zebrafish embryo. Development. 2001; 128:849–858. [PubMed: 11222140]

Beck CW, Whitman M, Slack JM. The role of BMP signaling in outgrowth and patterning of the Xenopus tail bud. Dev Biol. 2001; 238:303–314. [PubMed: 11784012]

Berg JN, Gallione CJ, Stenzel TT, Johnson DW, Allen WP, Schwartz CE, Jackson CE, Porteous ME, Marchuk DA. The activin receptor-like kinase 1 gene: genomic structure and mutations in hereditary hemorrhagic telangiectasia type 2. Am J Hum Genet. 1997; 61:60–67. [PubMed: 9245985]

Bharathy S, Xie W, Yingling JM, Reiss M. Cancer-associated transforming growth factor beta type II receptor gene mutant causes activation of bone morphogenic protein-Smads and invasive phenotype. Cancer Res. 2008; 68:1656–1666. [PubMed: 18339844]

Blank U, Seto ML, Adams DC, Wojchowski DM, Karolak MJ, Oxburgh L. An in vivo reporter of BMP signaling in organogenesis reveals targets in the developing kidney. BMC Dev Biol. 2008; 8:86. [PubMed: 18801194]

Chen YG, Hata A, Lo RS, Wotton D, Shi Y, Pavletich N, Massague J. Determinants of specificity in TGF-beta signal transduction. Genes Dev. 1998; 12:2144–2152. [PubMed: 9679059]

Chen YG, Massague J. Smad1 recognition and activation by the ALK1 group of transforming growth factor-β family receptors. J Biol Chem. 1999; 274:3672–3677. [PubMed: 9920917]

Choi M, Stottmann RW, Yang YP, Meyers EN, Klingensmith J. The bone morphogenetic protein antagonist noggin regulates mammalian cardiac morphogenesis. Circ Res. 2007; 100:220–228. [PubMed: 17218603]

Corish P, Tyler-Smith C. Attenuation of green fluorescent protein half-life in mammalian cells. Protein Eng. 1999; 12:1035–1040. [PubMed: 10611396]

Covassin LD, Siekmann AF, Kacergis MC, Laver E, Moore JC, Villefranc JA, Weinstein BM, Lawson ND. A genetic screen for vascular mutants in zebrafish reveals dynamic roles for Vegf/Plcg1 signaling during artery development. Dev Biol. 2009; 329:212–226. [PubMed: 19269286]

Daly AC, Randall RA, Hill CS. Transforming growth factor beta-induced Smad1/5 phosphorylation in epithelial cells is mediated by novel receptor complexes and is essential for anchorage-independent growth. Mol Cell Biol. 2008; 28:6889–6902. [PubMed: 18794361]

David L, Mallet C, Mazerbourg S, Feige JJ, Bailly S. Identification of BMP9 and BMP10 as functional activators of the orphan activin receptor-like kinase 1 (ALK1) in endothelial cells. Blood. 2007a; 109:1953–1961. [PubMed: 17068149]

David L, Mallet C, Vailhe B, Lamouille S, Feige JJ, Bailly S. Activin receptor-like kinase 1 inhibits human microvascular endothelial cell migration: potential roles for JNK and ERK. J Cell Physiol. 2007b; 213:484–489. [PubMed: 17620321]

Davis BN, Hilyard AC, Lagna G, Hata A. SMAD proteins control DROSHA-mediated microRNA maturation. Nature. 2008; 454:56–61. [PubMed: 18548003]

Deng Z, Morse JH, Slager SL, Cuervo N, Moore KJ, Venetos G, Kalachikov S, Cayanis E, Fischer SG, Barst RJ, Hodge SE, Knowles JA. Familial primary pulmonary hypertension (gene PPH1) is caused by mutations in the bone morphogenetic protein receptor-II gene. Am J Hum Genet. 2000; 67:737–744. [PubMed: 10903931]

Dennler S, Itoh S, Vivien D, ten Dijke P, Huet S, Gauthier JM. Direct binding of Smad3 and Smad4 to critical TGF beta-inducible elements in the promoter of human plasminogen activator inhibitor-type 1 gene. Embo J. 1998; 17:3091–3100. [PubMed: 9606191]

Dick A, Hild M, Bauer H, Imai Y, Maifeld H, Schier AF, Talbot WS, Bouwmeester T, Hammerschmidt M. Essential role of Bmp7 (snailhouse) and its prodomain in dorsoventral patterning of the zebrafish embryo. Development. 2000; 127:343–354. [PubMed: 10603351]

Dosch R, Gawantka V, Delius H, Blumenstock C, Niehrs C. Bmp-4 acts as a morphogen in dorsoventral mesoderm patterning in Xenopus. Development. 1997; 124:2325–2334. [PubMed: 9199359]

Faure S, de Santa Barbara P, Roberts DJ, Whitman M. Endogenous patterns of BMP signaling during early chick development. Dev Biol. 2002; 244:44–65. [PubMed: 11900458]

Feng XH, Derynck R. A kinase subdomain of transforming growth factor-beta (TGF-beta) type I receptor determines the TGF-beta intracellular signaling specificity. Embo J. 1997; 16:3912–3923. [PubMed: 9233801]

Feng XH, Derynck R. Specificity and versatility in tgf-beta signaling through Smads. Annu Rev Cell Dev Biol. 2005; 21:659–693. [PubMed: 16212511]

French CR, Erickson T, French DV, Pilgrim DB, Waskiewicz AJ. Gdf6a is required for the initiation of dorsal-ventral retinal patterning and lens development. Dev Biol. 2009; 333:37–47. [PubMed: 19545559]

Gaussin V, Van de Putte T, Mishina Y, Hanks MC, Zwijsen A, Huylebroeck D, Behringer RR, Schneider MD. Endocardial cushion and myocardial defects after cardiac myocyte-specific conditional deletion of the bone morphogenetic protein receptor ALK3. Proc Natl Acad Sci U S A. 2002; 99:2878–2883. [PubMed: 11854453]

Goumans MJ, Valdimarsdottir G, Itoh S, Lebrin F, Larsson J, Mummery C, Karlsson S, ten Dijke P. Activin receptor-like kinase (ALK)1 is an antagonistic mediator of lateral TGFbeta/ALK5 signaling. Mol Cell. 2003; 12:817–828. [PubMed: 14580334]

Goumans MJ, Valdimarsdottir G, Itoh S, Rosendahl A, Sideras P, ten Dijke P. Balancing the activation state of the endothelium via two distinct TGF-beta type I receptors. Embo J. 2002; 21:1743–1753. [PubMed: 11927558]

Gupta S, Zhu H, Zon LI, Evans T. BMP signaling restricts hemato-vascular development from lateral mesoderm during somitogenesis. Development. 2006; 133:2177–2187. [PubMed: 16672337]

Hao J, Ho JN, Lewis JA, Karim KA, Daniels RN, Gentry PR, Hopkins CR, Lindsley CW, Hong CC. In vivo structure-activity relationship study of dorsomorphin analogues identifies selective VEGF and BMP inhibitors. ACS Chem Biol. 2010; 5:245–253. [PubMed: 20020776]

Hata A, Lo RS, Wotton D, Lagna G, Massague J. Mutations increasing autoinhibition inactivate tumour suppressors Smad2 and Smad4. Nature. 1997; 388:82–87. [PubMed: 9214507]

Hauptmann G, Gerster T. Two-color whole-mount in situ hybridization to vertebrate and *Drosophila* embryos. Trends Genet. 1994; 10:266. [PubMed: 7940754]

Hild M, Dick A, Rauch GJ, Meier A, Bouwmeester T, Haffter P, Hammerschmidt M. The *smad5* mutation *somitabun* blocks Bmp2b signaling during early dorsoventral patterning of the zebrafish embryo. Development. 1999; 126:2149–2159. [PubMed: 10207140]

Hodge LK, Klassen MP, Han BX, Yiu G, Hurrell J, Howell A, Rousseau G, Lemaigre F, Tessier-Lavigne M, Wang F. Retrograde BMP signaling regulates trigeminal sensory neuron identities and the formation of precise face maps. Neuron. 2007; 55:572–586. [PubMed: 17698011]

Itoh S, ten Dijke P. Negative regulation of TGF-beta receptor/Smad signal transduction. Curr Opin Cell Biol. 2007; 19:176–184. [PubMed: 17317136]

Jadrich JL, O'Connor MB, Coucouvanis E. The TGF beta activated kinase TAK1 regulates vascular development in vivo. Development. 2006; 133:1529–1541. [PubMed: 16556914]

Jusuf PR, Harris WA. Ptf1a is expressed transiently in all types of amacrine cells in the embryonic zebrafish retina. Neural Dev. 2009; 4:34. [PubMed: 19732413]

Kang JS, Alliston T, Delston R, Derynck R. Repression of Runx2 function by TGF-beta through recruitment of class II histone deacetylases by Smad3. Embo J. 2005; 24:2543–2555. [PubMed: 15990875]

Kawakami K, Takeda H, Kawakami N, Kobayashi M, Matsuda N, Mishina M. A transposon-mediated gene trap approach identifies developmentally regulated genes in zebrafish. Dev Cell. 2004; 7:133–144. [PubMed: 15239961]

Kimmel CB, Ballard WW, Kimmel SR, Ullmann B, Schilling TF. Stages of embryonic development in the zebrafish. Dev Dynam. 1995; 203:253–310.

Klaus A, Saga Y, Taketo MM, Tzahor E, Birchmeier W. Distinct roles of Wnt/beta-catenin and Bmp signaling during early cardiogenesis. Proc Natl Acad Sci U S A. 2007; 104:18531–18536. [PubMed: 18000065]

Kofler B, Bulleyment A, Humphries A, Carter DA. Id-1 expression defines a subset of vimentin/S-100beta-positive, GFAP-negative astrocytes in the adult rat pineal gland. Histochem J. 2002; 34:167–171. [PubMed: 12495223]

Korchynskyi O, ten Dijke P. Identification and functional characterization of distinct critically important bone morphogenetic protein-specific response elements in the Id1 promoter. J Biol Chem. 2002; 277:4883–4891. [PubMed: 11729207]

Kramer C, Mayr T, Nowak M, Schumacher J, Runke G, Bauer H, Wagner DS, Schmid B, Imai Y, Talbot WS, Mullins MC, Hammerschmidt M. Maternally supplied Smad5 is required for ventral specification in zebrafish embryos prior to zygotic Bmp signaling. Dev Biol. 2002; 250:263–279. [PubMed: 12376102]

Kretzschmar M, Liu F, Hata A, Doody J, Massague J. The TGF-beta family mediator Smad1 is phosphorylated directly and activated functionally by the BMP receptor kinase. Genes Dev. 1997; 11:984–995. [PubMed: 9136927]

Kwan KM, Fujimoto E, Grabher C, Mangum BD, Hardy ME, Campbell DS, Parant JM, Yost HJ, Kanki JP, Chien CB. The Tol2kit: a multisite gateway-based construction kit for Tol2 transposon transgenesis constructs. Dev Dyn. 2007; 236:3088–3099. [PubMed: 17937395]

Lane KB, Machado RD, Pauciulo MW, Thomson JR, Phillips JA 3rd, Loyd JE, Nichols WC, Trembath RC. Heterozygous germline mutations in BMPR2, encoding a TGF-beta receptor, cause familial primary pulmonary hypertension. Nat Genet. 2000; 26:81–84. [PubMed: 10973254]

Liu D, Black BL, Derynck R. TGF-beta inhibits muscle differentiation through functional repression of myogenic transcription factors by Smad3. Genes Dev. 2001; 15:2950–2966. [PubMed: 11711431]

Liu F, Barral JM, Bauer CC, Ortiz I, Cook RG, Schmid MF, Epstein HF. Assemblases and coupling proteins in thick filament assembly. Cell Struct Funct. 1997; 22:155–162. [PubMed: 9113402]

Liu IM, Schilling SH, Knouse KA, Choy L, Derynck R, Wang XF. TGFbeta-stimulated Smad1/5 phosphorylation requires the ALK5 L45 loop and mediates the pro-migratory TGFbeta switch. Embo J. 2009; 28:88–98. [PubMed: 19096363]

Liu J, Stainier DY. Tbx5 and Bmp Signaling Are Essential for Proepicardium Specification in Zebrafish. Circ Res. 2010; 106

Liu W, Sun X, Braut A, Mishina Y, Behringer RR, Mina M, Martin JF. Distinct functions for Bmp signaling in lip and palate fusion in mice. Development. 2005; 132:1453–1461. [PubMed: 15716346]

Lo RS, Chen YG, Shi Y, Pavletich NP, Massague J. The L3 loop: a structural motif determining specific interactions between SMAD proteins and TGF-beta receptors. Embo J. 1998; 17:996–1005. [PubMed: 9463378]

Mandel EM, Kaltenbrun E, Callis TE, Zeng XX, Marques SR, Yelon D, Wang DZ, Conlon FL. The BMP pathway acts to directly regulate Tbx20 in the developing heart. Development. 2010; 137:1919–1929. [PubMed: 20460370]

Manning L, Ohyama K, Saeger B, Hatano O, Wilson SA, Logan M, Placzek M. Regional morphogenesis in the hypothalamus: a BMP-Tbx2 pathway coordinates fate and proliferation through Shh downregulation. Dev Cell. 2006; 11:873–885. [PubMed: 17141161]

Marques SR, Yelon D. Differential requirement for BMP signaling in atrial and ventricular lineages establishes cardiac chamber proportionality. Dev Biol. 2009; 328:472–482. [PubMed: 19232521]

McReynolds LJ, Gupta S, Figueroa ME, Mullins MC, Evans T. Smad1 and Smad5 differentially regulate embryonic hematopoiesis. Blood. 2007; 110:3881–3890. [PubMed: 17761518]

Mintzer KA, Lee MA, Runke G, Trout J, Whitman M, Mullins MC. *lost-a-fin* encodes a type I BMP receptor, Alk8, acting maternally and zygotically in dorsoventral pattern formation. Development. 2001; 128:859–869. [PubMed: 11222141]

Monteiro RM, de Sousa Lopes SM, Bialecka M, de Boer S, Zwijsen A, Mummery CL. Real time monitoring of BMP Smads transcriptional activity during mouse development. Genesis. 2008; 46 spcone.

Monteiro RM, de Sousa Lopes SM, Korchynskyi O, ten Dijke P, Mummery CL. Spatio-temporal activation of Smad1 and Smad5 in vivo: monitoring transcriptional activity of Smad proteins. J Cell Sci. 2004; 117:4653–4663. [PubMed: 15331632]

Muller F, Blader P, Rastegar S, Fischer N, Knochel W, Strahle U. Characterization of zebrafish smad1, smad2 and smad5: the amino-terminus of smad1 and smad5 is required for specific function in the embryo. Mech Dev. 1999; 88:73–88. [PubMed: 10525190]

Mullins MC, Hammerschmidt M, Kane DA, Odenthal J, Brand M, van Eeden FJ, Furutani-Seiki M, Granato M, Haffter P, Heisenberg CP, Jiang YJ, Kelsh RN, Nusslein-Volhard C. Genes establishing dorsoventral pattern formation in the zebrafish embryo: the ventral specifying genes. Development. 1996; 123:81–93. [PubMed: 9007231]

Nguyen VH, Schmid B, Trout J, Connors SA, Ekker M, Mullins MC. Ventral and lateral regions of the zebrafish gastrula, including the neural crest progenitors, are established by a bmp2b/swirl pathway of genes. Dev Biol. 1998; 199:93–110. [PubMed: 9676195]

Pannu J, Nakerakanti S, Smith E, ten Dijke P, Trojanowska M. Transforming growth factor-beta receptor type I-dependent fibrogenic gene program is mediated via activation of Smad1 and ERK1/2 pathways. J Biol Chem. 2007; 282:10405–10413. [PubMed: 17317656]

Park SO, Lee YJ, Seki T, Hong KH, Fliess N, Jiang Z, Park A, Wu X, Kaartinen V, Roman BL, Oh SP. ALK5- and TGFBR2-independent role of ALK1 in the pathogenesis of hereditary hemorrhagic telangiectasia type 2. Blood. 2008; 111:633–642. [PubMed: 17911384]

Payne-Ferreira TL, Yelick PC. Alk8 is required for neural crest cell formation and development of pharyngeal arch cartilages. Dev Dyn. 2003; 228:683–696. [PubMed: 14648845]

Persson U, Izumi H, Souchelnytskyi S, Itoh S, Grimsby S, Engstrom U, Heldin CH, Funa K, ten Dijke P. The L45 loop in type I receptors for TGF-beta family members is a critical determinant in specifying Smad isoform activation. FEBS Lett. 1998; 434:83–87. [PubMed: 9738456]

Pyati UJ, Cooper MS, Davidson AJ, Nechiporuk A, Kimelman D. Sustained Bmp signaling is essential for cloaca development in zebrafish. Development. 2006; 133:2275–2284. [PubMed: 16672335]

Roman BL, Pham VN, Lawson ND, Kulik M, Childs S, Lekven AC, Garrity DM, Moon RT, Fishman MC, Lechleider RJ, Weinstein BM. Disruption of acvrl1 increases endothelial cell number in zebrafish cranial vessels. Development. 2002; 129:3009–3019. [PubMed: 12050147]

Ross S, Hill CS. How the Smads regulate transcription. Int J Biochem Cell Biol. 2008; 40:383–408. [PubMed: 18061509]

Row RH, Kimelman D. Bmp inhibition is necessary for post-gastrulation patterning and morphogenesis of the zebrafish tailbud. Dev Biol. 2009; 329:55–63. [PubMed: 19236859]

Santoro MM, Pesce G, Stainier DY. Characterization of vascular mural cells during zebrafish development. Mech Dev. 2009; 126:638–649. [PubMed: 19539756]

Scheer N, Campos-Ortega JA. Use of the Gal4-UAS technique for targeted gene expression in the zebrafish. Mech Dev. 1999; 80:153–158. [PubMed: 10072782]

Shore EM, Xu M, Feldman GJ, Fenstermacher DA, Cho TJ, Choi IH, Connor JM, Delai P, Glaser DL, LeMerrer M, Morhart R, Rogers JG, Smith R, Triffitt JT, Urtizberea JA, Zasloff M, Brown MA, Kaplan FS. A recurrent mutation in the BMP type I receptor ACVR1 causes inherited and sporadic fibrodysplasia ossificans progressiva. Nat Genet. 2006; 38:525–527. [PubMed: 16642017]

Smith M, Hickman A, Amanze D, Lumsden A, Thorogood P. Trunk neural crest origin of caudal fin mesenchyme in the zebrafish Brachydanio rerio. Proc Biol Sci. 1994; 256:137–145.

Thisse, B.; Thisse, C. Fast Release Clones: A high throughput expression analysis. 2004. ZFIN direct data submission: http://zin.org

Toyama R, Chen X, Jhawar N, Aamar E, Epstein J, Reany N, Alon S, Gothilf Y, Klein DC, Dawid IB. Transcriptome analysis of the zebrafish pineal gland. Dev Dyn. 2009; 238:1813–1826. [PubMed: 19504458]

Upton PD, Davies RJ, Trembath RC, Morrell NW. Bone morphogenetic protein (BMP) and activin type II receptors balance BMP9 signals mediated by activin receptor-like kinase-1 in human pulmonary artery endothelial cells. J Biol Chem. 2009; 284:15794–15804. [PubMed: 19366699]

Urasaki A, Morvan G, Kawakami K. Functional dissection of the Tol2 transposable element identified the minimal cis-sequence and a highly repetitive sequence in the subterminal region essential for transposition. Genetics. 2006; 174:639–649. [PubMed: 16959904]

Verkhusha VV, Kuznetsova IM, Stepanenko OV, Zaraisky AG, Shavlovsky MM, Turoverov KK, Uversky VN. High stability of Discosoma DsRed as compared to Aequorea EGFP. Biochemistry. 2003; 42:7879–7884. [PubMed: 12834339]

Villefranc JA, Amigo J, Lawson ND. Gateway compatible vectors for analysis of gene function in the zebrafish. Dev Dyn. 2007; 236:3077–3087. [PubMed: 17948311]

Wang J, Sridurongrit S, Dudas M, Thomas P, Nagy A, Schneider MD, Epstein JA, Kaartinen V. Atrioventricular cushion transformation is mediated by ALK2 in the developing mouse heart. Dev Biol. 2005; 286:299–310. [PubMed: 16140292]

Wang Q, Wei X, Zhu T, Zhang M, Shen R, Xing L, O'Keefe RJ, Chen D. Bone morphogenetic protein 2 activates Smad6 gene transcription through bone-specific transcription factor Runx2. J Biol Chem. 2007; 282:10742–10748. [PubMed: 17215250]

Westerfield, M. The zebrafish book. Eugene: University of Oregon Press; 1995.

Wrighton KH, Lin X, Yu PB, Feng XH. Transforming Growth Factor {beta} Can Stimulate Smad1 Phosphorylation Independently of Bone Morphogenic Protein Receptors. J Biol Chem. 2009; 284:9755–9763. [PubMed: 19224917]

Yao LC, Blitz IL, Peiffer DA, Phin S, Wang Y, Ogata S, Cho KW, Arora K, Warrior R. Schnurri transcription factors from Drosophila and vertebrates can mediate Bmp signaling through a phylogenetically conserved mechanism. Development. 2006; 133:4025–4034. [PubMed: 17008448]

Yu PB, Hong CC, Sachidanandan C, Babitt JL, Deng DY, Hoyng SA, Lin HY, Bloch KD, Peterson RT. Dorsomorphin inhibits BMP signals required for embryogenesis and iron metabolism. Nat Chem Biol. 2008; 4:33–41. [PubMed: 18026094]

Zhao M, Qiao M, Oyajobi BO, Mundy GR, Chen D. E3 ubiquitin ligase Smurf1 mediates core-binding factor alpha1/Runx2 degradation and plays a specific role in osteoblast differentiation. J Biol Chem. 2003; 278:27939–27944. [PubMed: 12738770]

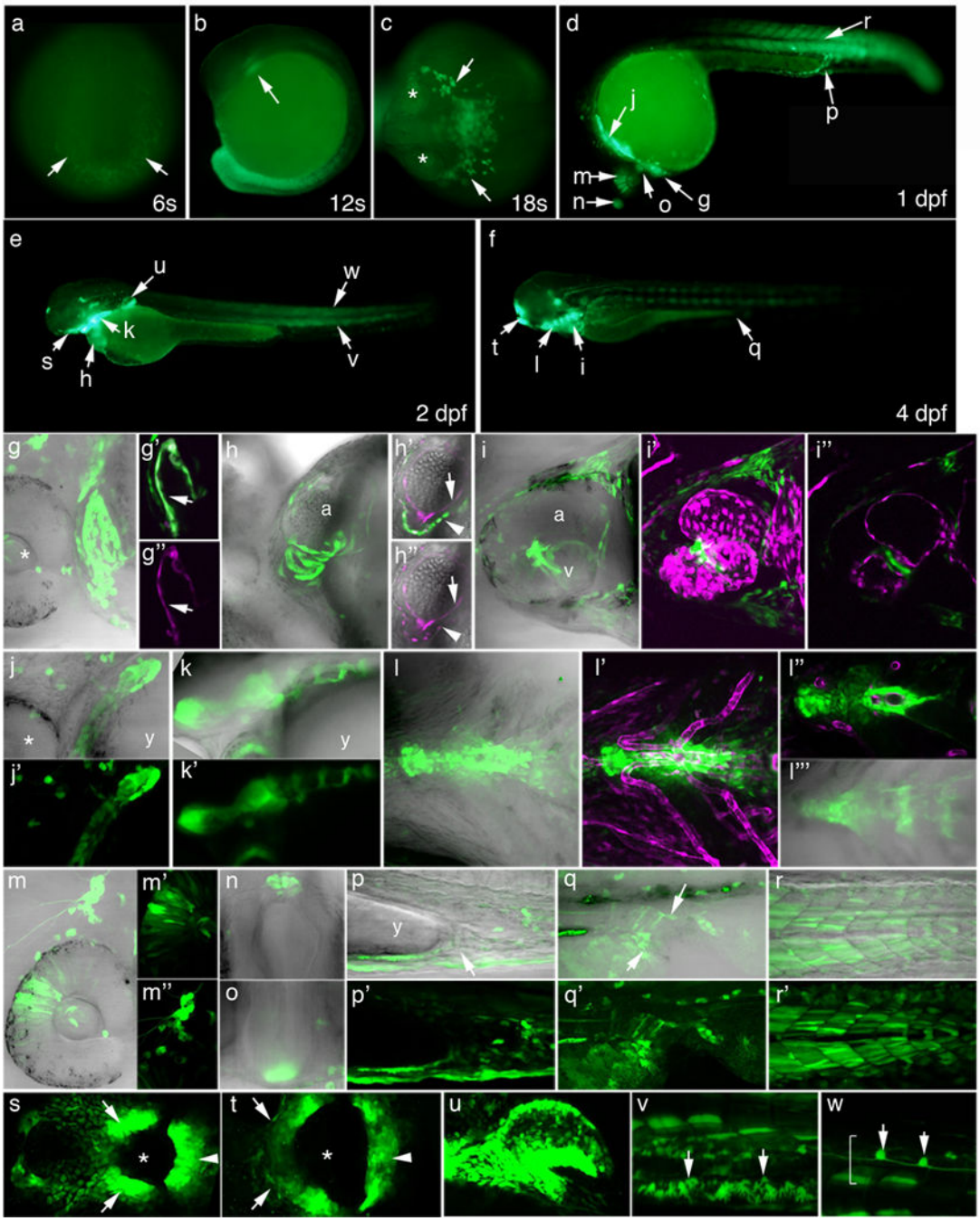

Figure 1. Developmental profile of pSmad1/5/8-mediated transcriptional activity in *Tg(bre:egfp)*^{pt510} embryos

In all images, green represents *bre*-driven EGFP expression. Magenta represents endothelial expression of *Tg(fli1ep:dsRedEx)*^{um13} or myocardial expression of *Tg(-5.1myl7:nDsRed2)*^{f2}, as noted below. (g–r, h′, h″, l‴) show fluorescence/transmission overlays. **(a-f)** Macro images. **(a)** 6 somites. Arrows point to tailbud. **(b)** 12 somites. Arrow points to myeloid progenitors. **(c)** 18 somites. Asterisks denote eyes; arrows point to myeloid cells. **(d–f)** Embryos at 1 **(d)**, 2 **(e)**, and 4 **(f)** dpf. Lettered arrows denote expression domains

highlighted in correspondingly lettered panels below. **(g–w)** 2D projections of confocal Z-series, except h′, h″, i″, and l″, which represent single optical sections extracted from the corresponding Z-series. Magnification = 400×. **(g–g″)** Heart at 1 dpf. Asterisk denotes eye. g′ and g″ are matched substacks showing EGFP/fli1ep:dsRedEx (overlay) and fli1ep:dsRedEx expression, respectively. Arrows denote endocardium. **(h–h″)** Heart at 2 dpf. h′ and h″ are matched optical sections of EGFP/ fli1ep:dsRedEx/-5.1myl7:nDsRed2 (overlay) and fli1ep:dsRedEx/-5.1myl7:nDsRed2. Arrows denote endocardium; arrowheads denote myocardium. **(i–i″)** Heart at 4 dpf. i′ and i″ show overlays of EGFP with fli1ep:dsRedEx, 2D projection and single optical section, respectively. **(j–j′)** Pharyngeal arches, 1 dpf. Asterisk denotes eye. **(k–k′)** Pharyngeal arches, 2 dpf. **(l–l‴)** Pharyngeal arches, 4 dpf. l′ and l″ show overlays of EGFP with fli1ep:dsRedEx, 2D projection and single optical section, respectively. l‴ shows substack of image shown in l. **(m–m″)** Dorsal retina (m′) and trigeminal ganglion (m″), 1 dpf. **(n)** Pineal gland, 1 dpf. **(o)** Hypothalamus, 1 dpf. **(p, p′)** Ventral mesenchyme and cloaca (arrow), 2 dpf. **(q, q′)** Cloaca, 4 dpf. Arrows delineate cloacal opening. **(r, r′)** Somites, 1 dpf. **(s)** Stomodeum, 2 dpf. Asterisk indicates presumptive mouth opening. Arrows indicate maxillary process; arrowhead, mandibular process. **(t)** Stomodeum, 4 dpf. Asterisk indicates open mouth; arrows indicate maxillary process; arrowhead, mandibular process. **(u)** Pectoral fin bud, 2 dpf. **(v)** Mesenchymal cells of the median finfold (arrows), 2 dpf. **(w)** Spinal cord neurons (arrows), 2 dpf. Spinal cord is bracketed. **(a)** Dorsoposterior view, posterior down. **(b, d–g, j, k, m, p–r, u–w)** Lateral view, anterior left, dorsal up. **(c)** Dorsal view, anterior left. **(h, i, l)** Ventral view, anterior left, left up. **(n)** Dorsal view, left to the right. **(o)** Frontal view, left to the right. **(s, t)** Frontal view, left up. Abbreviations: a = atrium; v = ventricle; y = yolk.

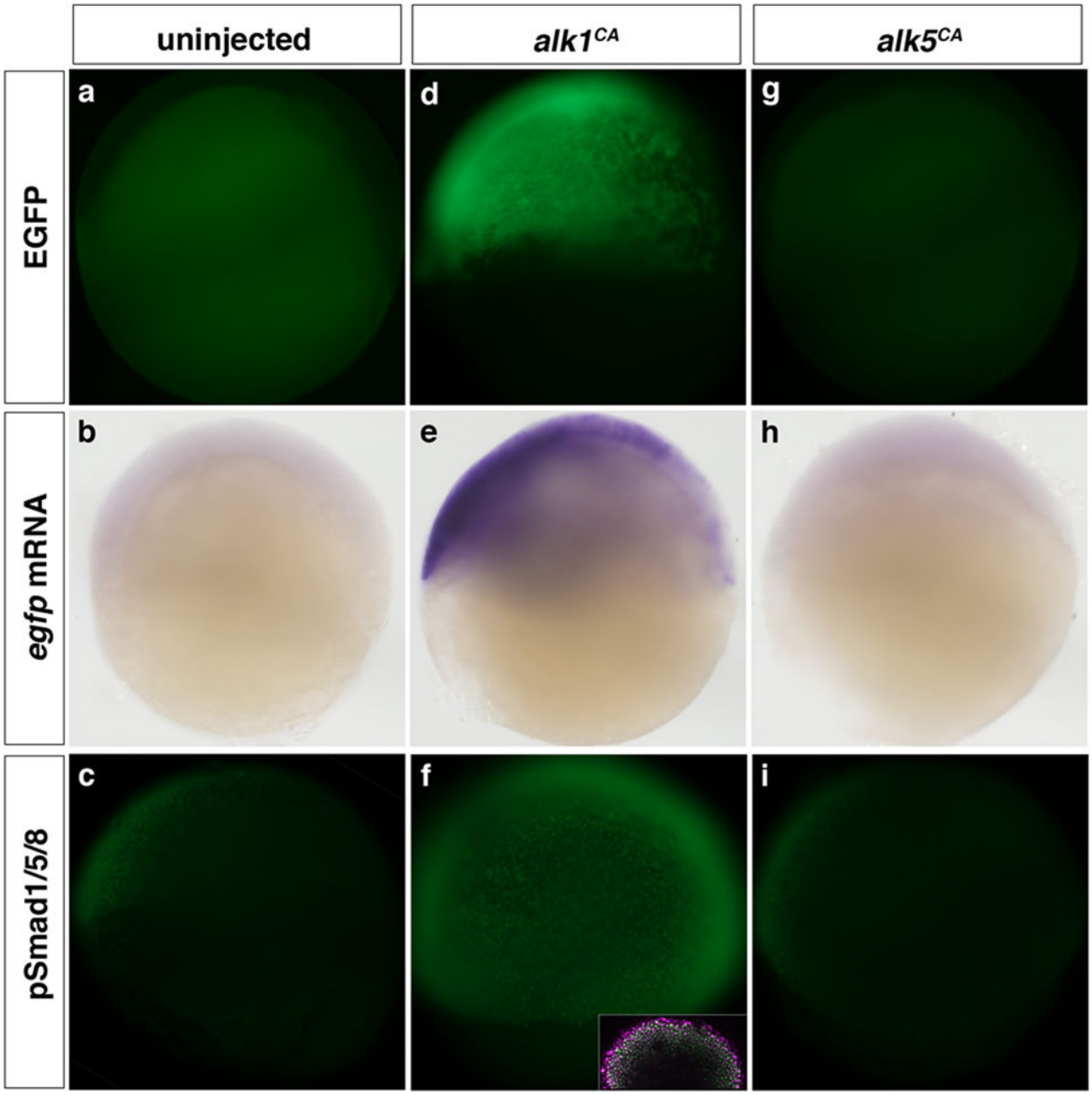

Figure 2. Expression of the *bre:egfp* transgene is responsive to changes in BMP type I signaling

Embryos were left uninjected **(a–c)** or injected with 5 pg *alk1*^{CA} mRNA **(d–f)** or 100 pg *alk5*^{CA} mRNA **(g–i)** at the one- to two-cell stage and assayed at shield stage (6 hpf). (**a, d, g**) Expression of *bre*-driven EGFP fluorescence in live embryos. (**b, e, h**) Expression of *bre*-driven e*gfp* mRNA assayed by in situ hybridization. (**c, f, i**) Expression of pSmad1/5/8 assayed by immunofluorescence. Inset in **f** is pSmad1/5/8 (green)/DAPI (magenta) merge. Lateral views, animal pole up, dorsal right. Original magnification 80× except insert, 200×.

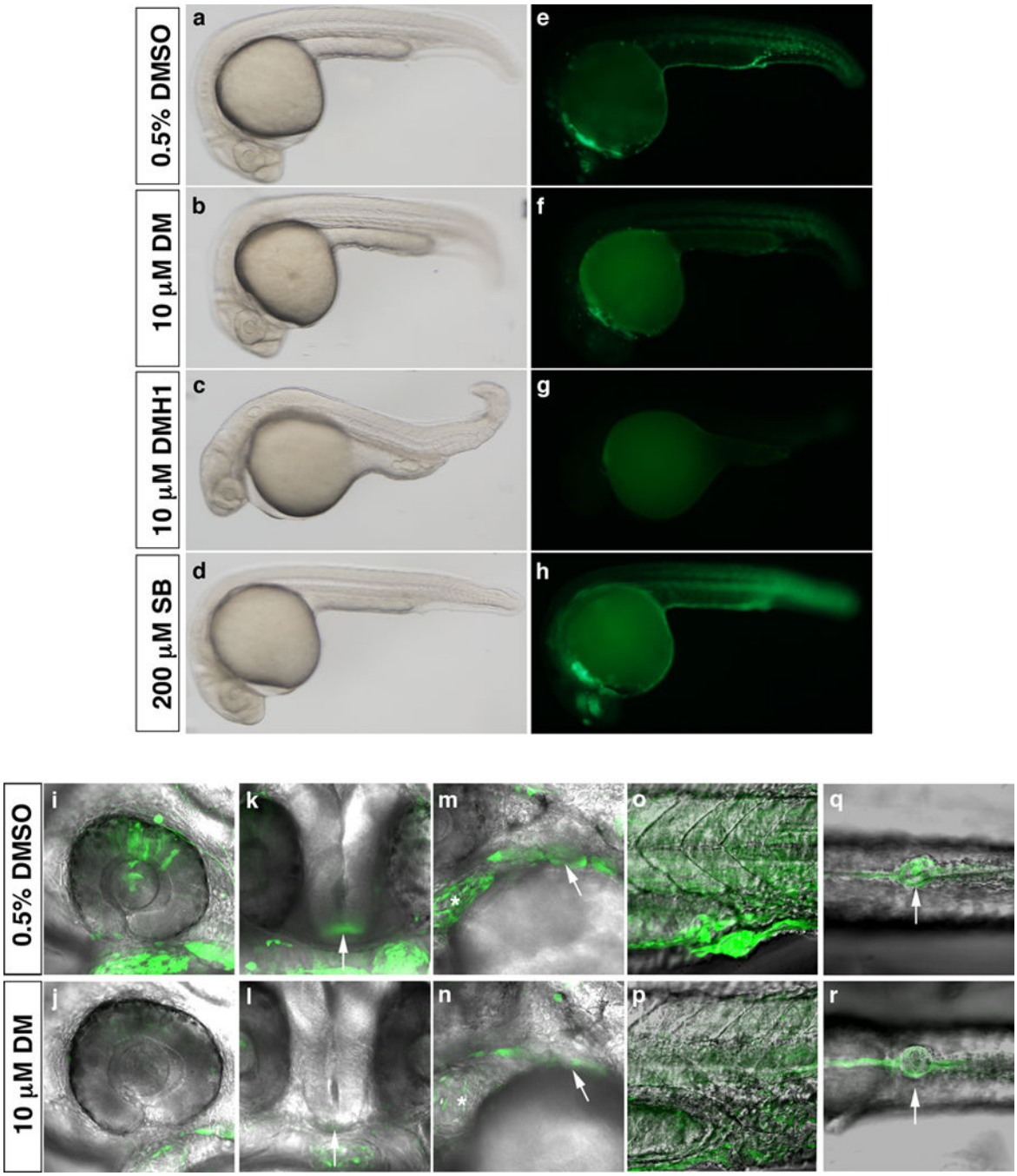

Figure 3. Expression of the *bre:egfp* transgene is globally downregulated by small molecule inhibition of BMP type I receptor-mediated Smad phosphorylation

Embryos were treated with either 0.5% DMSO **(a, e, i, k, m, o, q)**; 10 μM dorsomorphin (DM) **(b, f, j, l, n, p, r);** 10 μM DMH1 **(c, g)**, or 200 μM SB-431542 (SB) (**d, h**) between 10 and 24 hpf and imaged shortly after washout. In all images, green indicates *bre*-driven EGFP expression. Brightfield **(a–d)** and fluorescent **(e–h)** images, lateral view, anterior left, 80x magnification. **(i–r)** 2D projections of confocal Z-series showing EGFP and transmission overlays, 400× magnification. Expression domains shown include **(i, j)** retina;

(k, l) hypothalamus (arrow); **(m, n)** heart (asterisk) and pharyngeal arches (arrow); **(o, p)** somites; and **(q, r)** cloaca (arrow). **(i, j, m–p)** Lateral view, anterior left. **(k, l)** Frontal view, left is right. **(q, r)** Ventral view, anterior left.

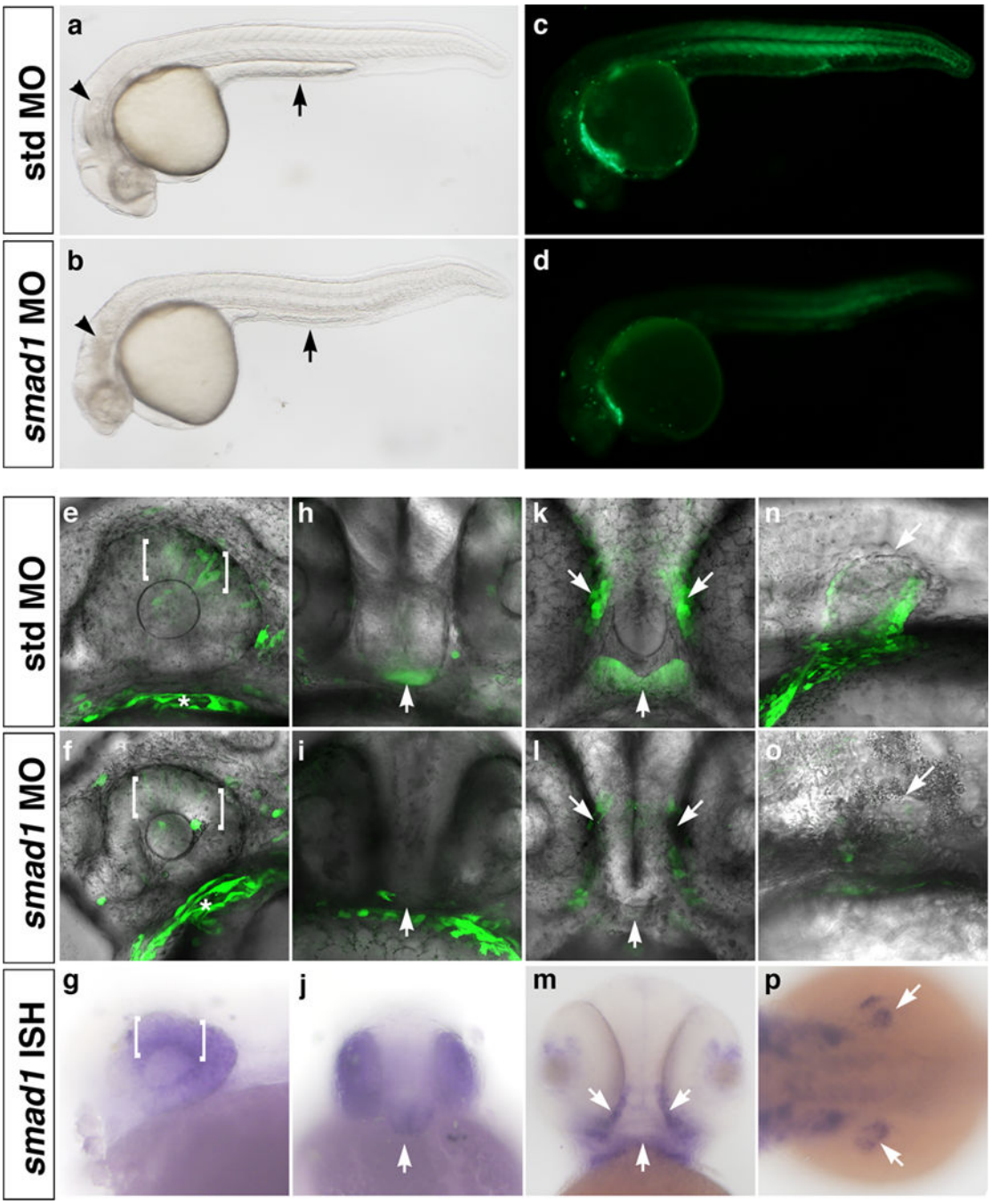

Figure 4. *smad1* knockdown downregulates *bre:egfp* transgene expression in *smad1*-expressing domains

Embryos were injected with 2 ng standard control morpholino **(a, c, e, h, k, n)** or 2 ng *smad1* morpholino **(b, d, f, i, l, o)** at the one- to two-cell stage. In all images, green indicates *bre*-driven EGFP expression. Brightfield **(a, b)** and fluorescent **(c, d)** images, lateral view, anterior left, 80× magnification. Note defects in yolk extension (arrow) in control embryo **(a)** versus *smad1* morphant **(b)**. **(e, f, h, i, k, l, n, o)** 2D projections of confocal Z-series showing EGFP and transmission overlays, 400× magnification. **(g, j, m, p)** Expression of

smad1 mRNA assayed by in situ hybridization. Expression domains shown include **(e–g)** dorsal retina (brackets), 1 dpf; **(h–j)** hypothalamus (arrow), 1 dpf; **(k–m)** stomodeum (arrows), 2 dpf; and **(n–p)** pectoral fin (arrows), 2 dpf. **(a–g, n, o)** Lateral view, anterior left. **(h–j)** Frontal view, left is right. **(k–m)** Ventral view, anterior up. **(p)** Dorsal view, anterior left.

Table 1

Sensitivity of *bre:egfp* expression to manipulation of Smad1/5 activity and expression

Expression domains	Dorsomorphin, 10 μM, 1 dpf	Smad5 MO, 2 ng, 1 dpf	Smad1 MO, 2 ng, 1 dpf	Smad1 MO, 2 ng, 2 dpf
Cloaca	++ (26%)	−/− (81%)	++ (63%)	NA
Heart	+ (76%)	− (96%)	−/− (86%)	− (99%)
Hypothalamus	++ (20%)	− (101%)	+ (74%)	NA
Median finfold	NA	NA	NA	++ (62%)
Pectoral fin	NA	NA	NA	++ (64%)
Pharyngeal arches	−/− (82%)	− (96%)	−/− (76%)	−/− (83%)
Pineal gland	−/− (81%)	− (95%)	−/− (86%)	NA
Retina	++ (52%)	+ (75%)	++ (47%)	NA
Somites/tailbud	−/− (82%)	++ (60%)	−/− (82%)	++ (58%)
Spinal cord neurons	NA	NA	NA	− (111%)
Stomodeum	NA	NA	NA	++ (42%)
Trigeminal ganglia	NA	NA	NA	− (99%)

[a] EGFP expression in individual embryos was subjectively scored by two independent observers as strong (3), moderate (2), weak (1) or not expressed (0), and scores averaged within control (0.5% DMSO for comparison to 10 μM dorsomorphin; 2 ng standard control morpholino for comparison to 2 ng *smad1* and *smad5* morpholinos) and experimental groups. Average scores for experimental groups are expressed as percent of control. Sensitivity to treatment was gauged as substantial (++, < 65% of control), moderate (+, 65–80% of control), minimal (−/−, 80–90% of control) or unaffected (−, > 90% of control). n = 24 per group for dorsomorphin treatment; 17 per group for *smad5* morpholino at 1 dpf; 27 per group for *smad1* morpholino at 1 dpf; and 24 per group for *smad1* MO at 2 dpf. Results are qualitatively reflective of 3–5 additional independent experiments. NA = not assessed.